Research Report

A growing degree day inference model based on mountain birch leaf cuticle analysis over a latitudinal gradient in Fennoscandia

Fabian EZ Ercan,[1] [ID] Hugo Jan De Boer[2]
and Friederike Wagner-Cremer[1]

Abstract

Cuticle analysis performed on fossil *Betula nana* (L.) leaves provides a strong proxy to reconstruct past growing season thermal properties expressed as growing degree days (GDD_5). This proxy is so far available for the dwarf birch only and, therewith, restricted to regions or past periods of subarctic climatic conditions. In this study, we analysed modern leaf samples of mountain birch (*Betula pubescens* spp. *czerepanovii* (N. I. Orlova) Hämet-Ahti), which has a wider temperature range than the dwarf birch *B. nana*. The strong latitudinal climate gradient over Fennoscandia provides a unique opportunity to track growing season temperature imprints in the epidermis cell morphology of the modern mountain birch. We quantified the GDD_5-dependent epidermal cell expansion, expressed as the undulation index (UI), over a 10° latitudinal transect translating to a range from ~1500°C to ~600°C GDD_5 in 2016. Our results indicate that even in mountain birch the UI is positively correlated to GDD_5 and, moreover, is largely independent of regional habitat conditions such as daylight length and precipitation. These results imply that in addition to the earlier studied (sub-)arctic dwarf birch, the closely related mountain birch can also be utilized in GDD_5 reconstructions. The abundant presence of fossil mountain birch leaves in sediments from warmer than (sub) arctic palaeoclimates enables the reconstruction of growing season climate dynamics over past phases of climate change, overcoming earlier restrictions of the proxy related to spatial and temporal species occurrence as well as local light regimes.

Introduction

Palaeobotanical proxies based on cuticle properties are increasingly implemented to reconstruct environmental and climatic changes by quantifying leaf morphological adaptations in response to environmental changes. The variety of proxies available to date enable atmospheric CO_2 reconstructions (McElwain and Steinthorsdottir, 2017; Royer, 2001; Wagner-Cremer et al., 2004), estimates of transpiration changes (Bodin et al., 2013; De Boer et al., 2011; Franks and Beerling, 2009; Lammertsma et al., 2011), drought stress signals (Wagner-Cremer et al., 2007) and volcanic SO_2 pollution (Steinthorsdottir et al., 2018). Microphenological studies have further demonstrated that the growing season thermal conditions also result in distinct imprints in the leaf epidermal cell morphology (Wagner-Cremer et al., 2010).

Microphenological proxies for growing season dynamics through time are of interest, as ongoing global warming causes a significant lengthening of the growing season in large parts of the Northern Hemisphere, altering the spring phenology of woody plants (Flynn and Wolkovich, 2018; Polgar and Primack, 2011; Zohner and Renner, 2014). The physiological response of plants in return has the potential to alter the physical and biological properties of large vegetated land areas influencing local and regional climatic conditions through albedo and transpiration feedback (Bonan, 2008; Lian et al., 2018; Piao et al., 2017).

In this context, growing season climate reconstructions provide a powerful tool for determining seasonality dynamics during natural climate change on various spatiotemporal scales (Finsinger et al., 2013; Wagner-Cremer and Lotter, 2011). The leaf cuticle analysis-based proxy, quantifying the growing season thermal properties, relies on the maturation stage of leaf epidermal cells reached under the cumulative growing degree days (GDD) during the annual growth period (Wagner-Cremer et al., 2010). The leaf epidermal cell expansion follows an ontogenetic succession, in which cell size and cell wall sinuosity increase during the leaf maturation period (Kürschner et al., 1996; Wagner-Cremer et al., 2007, 2010). The maturation stage of the epidermal cells is expressed as the undulation index (UI), which quantifies the degree of cell wall sinuosity over cell area (CA) (Kürschner et al., 1996). This proxy was originally introduced to identify light intensity-related leaf morphotypes in closed canopy species such as oak (Kürschner et al., 1996). In open canopy trees and shrubs such as *Betula*, however, the undulation occurring in epidermal cells is strongly related to the duration and temperature available to plants during the growth period (Wagner-Cremer et al., 2010).

[1]Palaeoecology, Department of Physical Geography, Utrecht University, The Netherlands
[2]Copernicus Institute of Sustainable Development, Department of Environmental Sciences, Utrecht University, The Netherlands

Corresponding author:
Fabian EZ Ercan, Palaeoecology, Department of Physical Geography, Utrecht University, Princetonlaan 8a, 3584 CB Utrecht, The Netherlands.
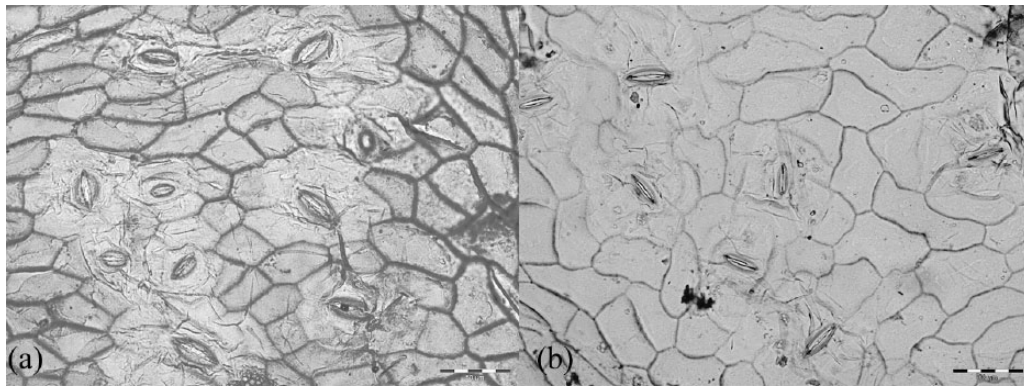Email: f.e.z.ercan@uu.nl

Figure 1. Representative images of mountain birch cuticles grown under (a) 776 GDD$_5$ and (b) 1493 GDD$_5$, showing stomata bearing alveole areas and epidermal cells with low and high cell wall undulation, respectively. Scale bar is 50 μm.

A distinct correlation between the UI of the (sub-)arctic dwarf birch *Betula nana* and GDD$_5$ (the growing season cumulative sum of degree Celsius above 5°C) was first established through continuous leaf monitoring ongoing since 1996 at the Subarctic Research Station site in Kevo, northern Finland (Wagner-Cremer et al., 2010). The robustness of the available UI inference model as GDD$_5$ proxy was subsequently tested by comparison of UI values from fossil *B. nana* leaf cuticles preserved in Scandinavian peat deposits with historical GDD$_5$ records (Finsinger et al., 2013; Wagner-Cremer et al., 2010). A first application to Late Glacial *B. nana* cuticles has further shown the applicability to Quaternary periods of rapid climate change (Wagner-Cremer and Lotter, 2011).

Although the potential value of the UI as a GDD$_5$ proxy to support spatiotemporal analysis of seasonality changes has been demonstrated, the proxy is currently tested only for the (sub-)arctic dwarf birch. In order to apply this proxy on a broader spatial and temporal scale, additional modern species with more southern geographical ranges are needed to overcome the limits of the GDD$_5$ inference model for *B. nana* with its relatively narrow temperature range.

Moreover, potential sources of reconstruction uncertainties have to be evaluated. A point of discussion is thereby the influence of photoperiod (PP) on leaf phenology under changing temperatures (Flynn and Wolkovich, 2018; Körner and Basler, 2010; Zohner et al., 2016). This study focuses on the Scandinavian mountain birch (*Betula pubescens* spp. *czerepanovii* (N. I. Orlova) Hämet-Ahti), which groups the introgressive hybrids between the downy birch (*B. pubescens* Ehrh.) and the dwarf birch (*B. nana* L.) (Vaarama and Valanne, 1973; Wagner-Cremer et al., 2000). The mountain birch contributes large proportions to the Fennoscandian broadleaved forests and occurs over the climatic gradient from cold-temperate to subarctic conditions. Over this geographic range, the cold-adapted dwarf birch is successively replaced by the thermophilous mountain birch, therewith providing an opportunity to extend GDD$_5$ and PP ranges to more warmer climates in lower latitudes. Cuticle analysis of the different birch species and hybrids has already revealed distinct and specific morphological characteristics of mountain birch and dwarf birch, which allows to distinguish mountain birch from dwarf birch in fossil leaf samples (Wagner-Cremer et al., 2000). In this study, we therefore aim to expand and validate the UI proxy for growing season thermal properties by quantifying the sensitivity of mountain birch to the GDD$_5$ range occurring over a 10° latitudinal gradient in Scandinavia.

Materials and methods

Leaf sampling

The leaf sampling campaign was carried out in 2016 at the end of the growing season (24–30 September), when trees showed autumn colours indicating leaf senescence. We sampled 20 randomly selected mountain birch leaves per site at 28 locations in Finland and northern Norway (Figure 2), with a spacing of approximately 100 km between sites.

Microscopic analysis

From 26 locations, three to five leaves were analysed. Sections of 0.5×0.5 cm^2 from individual leaves were bleached in sodium hypochlorite (<5%) at room temperature for 12–24 h. The lower cuticle was subsequently removed and stained with safranin. Permanent microscopic slides were made using glycerine jelly. Five digital photographs of each cuticle were taken using a Leica Quantimet 500 C/500+ microscope and AnalySIS image analysis software (AnalySIS auto 5.1) at 1000× magnification. Analysis of epidermal and stomatal cell properties was performed using ImageJ 1.52a. Two representative cuticle images with low and high UI are shown in Figure 1.

To estimate the mean epidermal CA (μm2) and epidermal cell circumference (CC; (μm), 30 random pavement cells per sample were analysed, avoiding cells over venation and leaf margins. From CA and CC, the UI (dimensionless) of the epidermal cell wall was calculated following Kürschner (1997) as

$$\text{UI[dimensionless]} = \frac{CC}{2\pi \cdot \sqrt{CA / \pi}}$$

Meteorological data

To compare the cuticle analysis results with meteorological data, the measured daily average temperature and precipitation data of the weather station nearest to each individual sampling site was extracted from the KNMI Explorer database (Van Oldenborgh et al., 2009).

GDD$_5$ was calculated from daily temperatures recorded throughout the growing season. GDD covers the growing potential for vegetation in a given year and is expressed by the cumulative sum of degrees Celsius above a determined base temperature (McMaster and Wilhelm, 1997; Weijers et al., 2013) as

$$\text{GDD}_X = \sum_{i=1}^{274} (T_i - X), \quad T_i \geq X$$

where Ti is the daily mean temperature for day i and X is the selected threshold temperature in degrees Celsius. For Ti, the daily mean temperature from each station was used. For the latitudinal range covered in this study, 5°C is the commonly used threshold temperature for plant growth and was taken as threshold temperature X, resulting in GDD$_5$ (Carter, 1998). The sum of GDD$_5$ was calculated from 1 January 2016 to 30 September 2016.

May through September (MJJAS) temperature and precipitation data were used to calculate average spring and summer conditions. Average winter temperature and precipitation were calculated from November, December 2015 as well as January, February and March 2016 (NDJFM). We note that the long summer and winter definitions were necessary to cover the growing season of the southernmost sample locations. Average precipitation and the total precipitation sum were calculated as 1 October 2015 until 30 September 2016, representing the total amount of precipitation since shedding of the leaves in the previous season to senescence of the current leaf sample set. PP was defined as the cumulative sunlight hours at the latitude of each sample location between March and September.

Spatial analysis

To visualize spatial variability in GDD_5 and UI, inverse distance-weighted interpolation (Shepard, 1964) was performed using the '*idw()*' function in the *gstat* package (Gräler et al., 2016) in R version 3.5.2 (R Core Team, 2019). A maximum search radius of 100 km was set based on the sampling distance, and the inverse distance-weighting power was set to 2. This resulted in a root-mean-square deviation of 0.02 for UI and 95.09 for GDD_5 (as determined from leave-one-out cross-validation). For management and visualization of spatial data in R, the *rgdal* (Bivand et al., 2018), *raster* (Hijmans, 2018) and *sp* (Bivand et al., 2013; Pebesma and Bivand, 2005) packages were used. Country basemaps were retrieved from the *ggplot2* package (Wickham, 2016).

GDD_5 inference model

Linear least-square regression was used to relate measured UI values to known GDD_5 across all sampling localities. For the prediction of past $GDD_{5\,fossil}$ from UI obtained from fossil leaf material (UI_{fossil}) values, it is necessary to inverse the original least-squares regression function $[UI] = a[GDD_5] + b$. The inverse of the fit results in $[GDD_{5\,fossil}] = [UI_{fossil}](1/a) - (b/a)$ and minimizes the error towards the original modern *y*-variable (UI), with *x*-variable (GDD_5) as fixed measurement. A Monte Carlo simulation (1000 times repetition) based on the mean UI values for each locality was used to test the reliability of the inference model, each time with a random division of the dataset in two halves, a reference and a test part, generating averages and uncertainty ranges in the slope (a) and intercept (b) for the inference model function.

Independent test data

To additionally test the predictive capacity of the inference model, GDD_5 values were inferred from an independent dataset of UI values measured on mountain birch leaves collected in 1997 at several Finnish sites between 62°N and 70°N (Table 1), including samples published in Wagner-Cremer et al. (2000). The leaf material was sampled and analysed, applying the same protocol as for the samples collected in 2016. For the five Finnish localities, instrumental GDD_5 data for 1997 (Van Oldenborgh et al., 2009) are available, with which the inferred GDD_5 values are compared.

Results

An inverse distance-weighted interpolation of the data has been used to visualize the spatial distribution of GDD_5 and UI values, respectively (Figure 2). The GDD_5 data from the meteorological observations range from 1493 GDD_5 to 578 GDD_5 over the latitudinal gradient from 60.7°N to 69.9°N (Figure 2a and b). UI values range from 1.12 to 1.27 over the same latitudinal gradient (Figure 2c and d). GDD_5 and UI thereby show strong linear negative relations to latitude $R_2 = 0.88$ and $R_2 = 0.69$, respectively.

The UI of the 2016 latitudinal transect has been tested against latitude, winter temperature, winter precipitation, summer temperature, summer precipitation, GDD_5 and PP of the growing season (Table 2).

GDD_5 inference model

We developed our GDD_5 inference model based on site-averaged UI values obtained from the 2016 transect together with meteorological observations of GDD_5 along this transect (Figure 3a). Using inverse regression, we obtained the linear function $[GDD_5] = 7744.8[UI] - 8086.8$ ($R^2 = 0.77$, $p < 0.001$). The 95% confidence intervals of the slope and intercept of the GDD_5 inference model are 6178.4 to 1017.1, and -1089.8 to -6244.2, respectively.

To test the predictive skills and accuracy of the inference model, independent UI data from a transect with a similar latitudinal range (62.4°N–69.9°N) collected in 1997 with known GDD_5 at growth locality have been run through the inference model (Figure 3b). There is some minor offset in slope and intercept between the hypothetical control line ($y = x$) and the linear model ($y = 1.1219 \times -207.7$) fitted through the predicted values and their corresponding observed values predicting the value of the inference model is high ($R^2 = 0.86$, $p = 0.02$).

Discussion

UI sensitivity to GDD_5

Local GDD_5 values explain 77% of the UI variability in a highly significant linear relation over the range from 578 to 1493 GDD_5 and thus corroborate the proposed concept that growing season thermal properties produce a strong, detectable imprint in the leaf morphology in open canopy species (Wagner-Cremer et al., 2010). The data thereby show that this adjustment in epidermal cell morphology not only occurs in the subarctic dwarf birch *B. nana*, but is also present in mountain birch. The mountain birch is closely related to the dwarf birch and originates from hybridization between *B. nana* and *B. pubescens* (Vaarama and Valanne, 1973; Wagner-Cremer et al., 2000) under current climatic conditions in the northern high latitudes. Fossil hybrid forms are difficult to recognize, but are likely to have occurred under past climate changes, too (Wagner-Cremer et al., 2000). Testing of cuticle characteristics in *B. nana, B. pubescens* and various mountain birch hybrids grown in the treeline arboretum at Kevo subarctic research station (Utjoki, Finland) has shown, however, that mountain birch varieties can be treated as a single group, since no significant differences in UI or other cuticle characteristics have been found (Wagner-Cremer et al., 2000). The separation between mountain birch and *B. nana* in fossil, fragmented material is relatively easy through either leaf margin analysis or, if marginal parts are not available, via determination of the stomatal length, which is significantly lower in *B. nana* than in the mountain birch group (Wagner-Cremer et al., 2000).

The validity of the mountain birch inference model is supported by an independent sample set collected in 1997 from localities with instrumental GDD_5 data. The response rate of the UI in mountain birch to GDD_5 is, moreover, highly comparable to the relation determined for *B. nana*, with UI changes of approximately 0.02–0.03 (UI) per 100°C GDD_5 based on the currently available GDD_5 ranges of the individual inference models.

Effects of PP and precipitation

Our results also revealed a significant negative correlation between PP and UI. PP is a globally unidirectional parameter associated to latitude, which determines the amount of daylight available during the growth period of the plants, and which can
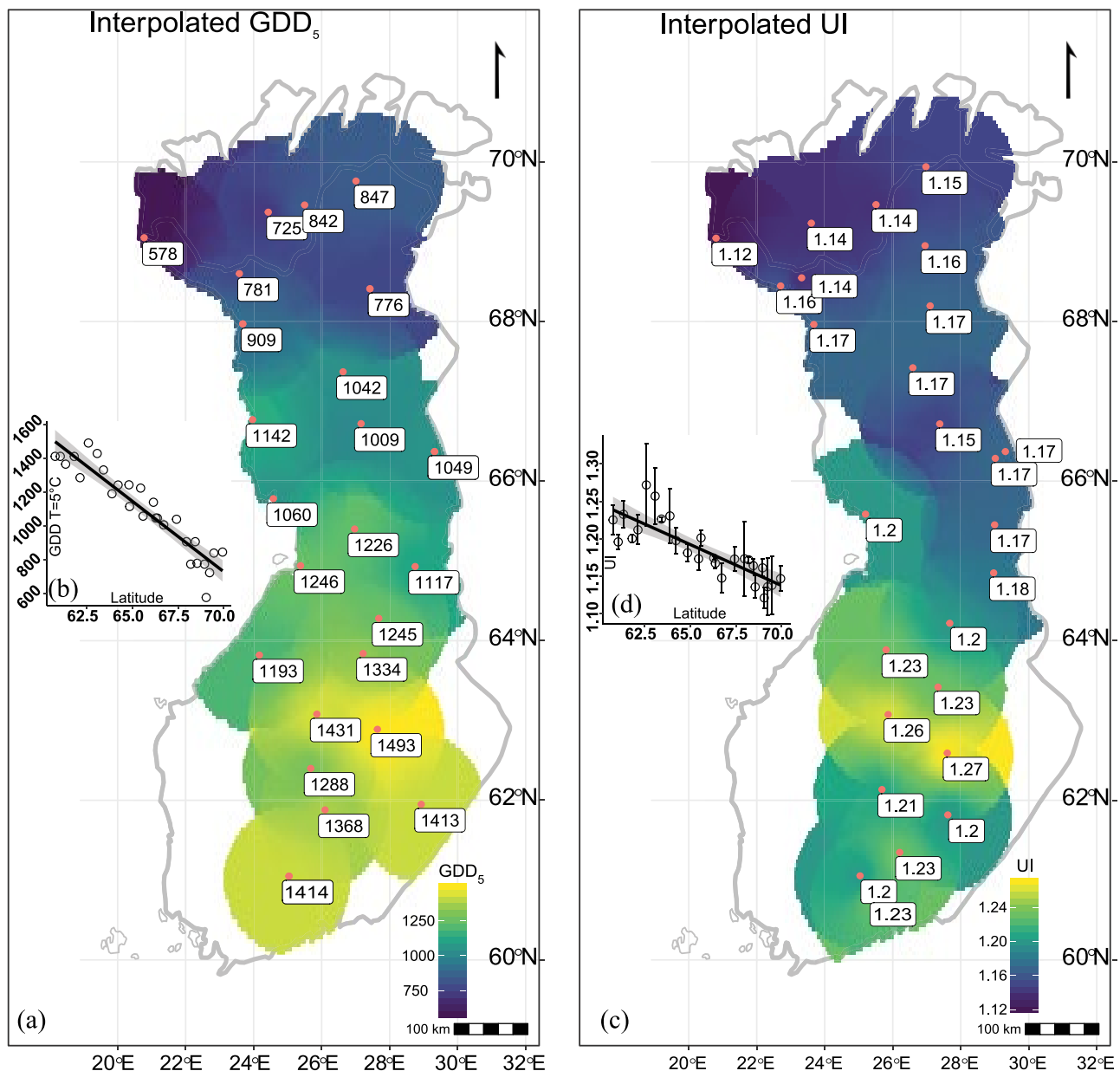
Figure 2. (a) Meteorological station locations (*n* = 28) and their measured GDD$_5$ values, with inverse distance-weighted interpolation gradient. (b) Linear relation between latitude and GDD$_5$. (c) Sample locations and the measured mountain birch UI values (*n* = 26) with inverse distance-weighted interpolation gradient. (d) Linear relation between latitude and UI with error bars indicating the naturally occurring variance in UI.

Table 1. Test samples of mountain birch leaves collected in 1997.

Locality	Latitude °N	UI	GDD$_5$ 1997
Mekrijärvi, Finland	62.4	1.24 ± 0.02	1498
Oulu, Finland	65.0	1.18 ± 0.03	1195
Peera, Finland	69.0	1.17 ± 0.02	760
Kevo 2, Finland	69.5	1.17 ± 0.02	765
Kevo 1, Finland	69.9	1.15 ± 0.02	745

UI: undulation index; GDD: growing degree days.

be especially critical at the start of the season. The mountain birch is a typical pioneer species that occurs in the early vegetation succession. Phenological observations of pioneer species such as birch, hazel or poplar show that onset of leaf growth is insensitive to PP in spring and that budburst and leaf growth are thus predominantly regulated by temperature (Körner and Basler,

2010; Polgar and Primack, 2011). Earlier studies on the effects of PP on *B. pubescens* show that in experimental set-ups, increased PP under set temperature leads to increasing leaf size and numbers (Habjørg, 1971). This photoperiodic response, however, is suppressed when plants are exposed to low temperatures overruling the positive effect of prolonged daylight availability (Habjørg, 1971). These findings support our hypothesis that the UI in mountain birch is not directly linked to daylight length, but that the determined correlation rather reflects a false signal resulting from the co-occurring, but unrelated latitudinal changes in GDD$_5$ and PP.

A strong latitudinal precipitation gradient occurs over Scandinavia, where southern and eastern Finland receive nearly twice as much precipitation as the northern region of Lapland. Our data show high correlation values for the UI and winter precipitation, but no correlation of UI with summer precipitation. Winter precipitation of the studied year clearly follows the general latitudinal precipitation gradient as is evident from the high negative

Table 2. Epidermal characteristics and meteorological data (correlation coefficents (*R* value) and coefficient of determination (*R*^{2} value) are given in parenthesis).

	UI	Latitude	Temp NDJFM	Precip NDJFM	Temp MJJAS	Precip MJJAS	GDD$_5$	PP MAMJJAS
UI	X	−0.83 (0.69)***	0.86 (0.74)***	0.78 (0.61)***	0.79 (0.62)***	n.s.	0.88 (0.77)***	−0.85 (0.72)***
Latitude	−0.83 (0.69)***	X	−0.97 (0.94)***	−0.89 (0.79)***	−0.97 (0.94)***	−0.89 (0.79)***	−0.94 (0.88)***	1***
GDD$_5$	0.88 (0.77)***	−0.94 (0.88)***	0.92 (0.85)***	0.82 (0.67)***	0.89 (0.79)***	−0.36 (0.13)*	X	−0.95 (0.90)***

UI: undulation index; NDJFM: November, December 2015 and January, February and March 2016; MJJAS: May through September; GDD: growing degree days; PP: photoperiod; n.s.: not significant.
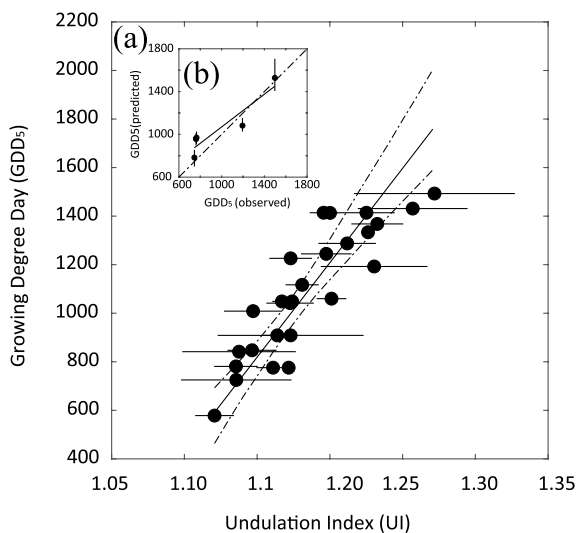***$p < 0.001$. *$p < 0.1$.

Figure 3. (a) Inference model fit showing the relation between GDD$_5$ and UI of mountain birch obtained from the 2016 transect. Round markers indicate UI sample means and horizontal error bars indicate one standard deviation around the sample mean. The solid and dashed lines show the mean model fit with 95% confidence intervals. (b) Independent inference model test based on leaves collected in 1997 at five localities in Scandinavia. Round markers indicate observed versus predicted GDD$_5$ inferred using the 2016 inference model. Vertical error bars indicate 95% confidence intervals around the predicted GDD$_5$. The solid line is the linear regression ($R^2 = 0.86$, $p = 0.24$), and the dashed line represents a hypothetical 1:1 relation between predicted and observed GDD$_5$ values.

correlation between these two variables. The winter precipitation is predominantly received as snow and, thus, does not directly affect the leaf growth after snowmelt. The lack of correlation with the summer precipitation, on the contrary, corroborates earlier findings from a single-site study from Kevo, Lapland, where continuous time series analysis over the period from 1975 to 2008 did not reveal any significant imprint of May–September precipitation in the UI of *B. nana* (Wagner-Cremer et al., 2010). Nonetheless, water deficit has the potential to reduce epidermal cell expansion (Wagner-Cremer et al., 2010) and throughout individual growing seasons may well have a growth-restricting effect, an aspect that needs careful consideration and additional testing.

Our results support the GDD$_5$ inference model for mountain birch as a valuable addition to the proxy so far restricted to *B. nana*. By adding mountain birch, the temperature range over which the proxy can be applied is expanded and now covers growing season temperature regimes characteristic of boreal forest biomes rather than (sub-)arctic conditions only. Spring season reconstructions based on cuticle analysis thus become possible also for sites and localities where the fossil leaf assemblages either include climatic warming phases with vegetation successions or for leaf bearing sequences in geographical regions outside the climatic prerequisites of the (sub-)arctic dwarf birch.

ORCID iD

Fabian EZ Ercan https://orcid.org/0000-0001-6231-4345

References

Bivand R, Keitt T and Rowlingson B (2018) rgdal: Bindings for the 'geospatial' data abstraction library. Available at: https://cran.r-project.org/package=rgdal.

Bivand RS, Pebesma E and Gomez-Rubio V (2013) *Applied Spatial Data Analysis with R*. New York: Springer.

Bodin PE, Gagen M, McCarroll D et al. (2013) Comparing the performance of different stomatal conductance models using modelled and measured plant carbon isotope ratios (δ13C): Implications for assessing physiological forcing. *Global Change Biology* 19(6): 1709–1719.

Bonan GB (2008) Forests and climate change: Forcings, feedbacks, and the climate benefits of forests. *Science* 320(5882): 1444–1449.

Carter TR (1998) Changes in the thermal growing season in Nordic countries during the past century and prospects for the future. *Agricultural and Food Science* 7(2): 161–179.

De Boer HJ, Lammertsma EI, Wagner-Cremer F et al. (2011) Reply to Miglietta et al.: Maximal transpiration controlled by plants. *Proceedings of the National Academy of Sciences of the United States of America* 108(28): E276.

Finsinger W, Schoning K, Hicks S et al. (2013) Climate change during the past 1000 years: A high-temporal-resolution multiproxy record from a mire in northern Finland. *Journal of Quaternary Science* 28(2): 152–164.

Flynn DFB and Wolkovich EM (2018) Temperature and photoperiod drive spring phenology across all species in a temperate forest community. *New Phytologist* 219(4): 1353–1362.

Franks PJ and Beerling DJ (2009) Maximum leaf conductance driven by CO$_2$ effects on stomatal size and density over geologic time. *Proceedings of the National Academy of Sciences of the United States of America* 106(25): 10343–10347.

Gräler B, Pebesma E and Heuvelink G (2016) Spatio-temporal interpolation using gstat. *RFID Journal* 8(1): 204–218.

Habjørg A (1971) Effects of photoperiod and temperature on growth and development of three latitudinal and three altitudinal populations of Betula pubescens EHRH. *Meldinger fra Norges landbrukshøgskole* 44(26): 1–27.

Hijmans RJ (2018) raster: Geographic data analysis and modeling. Available at: https://cran.r-project.org/web/packages/raster/index.html.

Körner C and Basler D (2010) Plant science: Phenology under global warming. *Science* 327(5972): 1461–1462.

Kürschner WM (1997) The anatomical diversity of recent and fossil leaves of the durmast oak (Quercus petraea Lieblein/Q. pseudocastanea Goeppert) – Implications for their use as biosensors of palaeoatmospheric CO_2 levels. *Review of Palaeobotany and Palynology* 96: 1–30.

Kürschner WM, Van der Burgh J, Visscher H et al. (1996) Oak leaves as biosensors of late neogene and early pleistocene paleoatmospheric CO2 concentrations. *Marine Micropaleontology* 27(1–4): 299–312.

Lammertsma EI, De Boer HJ, Dekker SC et al. (2011) Global CO_2 rise leads to reduced maximum stomatal conductance in Florida vegetation. *Proceedings of the National Academy of Sciences of the United States of America* 108(10): 4035–4040.

Lian X, Piao S, Huntingford C et al. (2018) Partitioning global land evapotranspiration using CMIP5 models constrained by observations. *Nature Climate Change* 8(7): 640–646.

McElwain JC and Steinthorsdottir M (2017) Paleoecology, ploidy, paleoatmospheric composition, and developmental biology: A review of the multiple uses of fossil stomata. *Plant Physiology* 174(2): 650–664.

McMaster GS and Wilhelm WW (1997) Growing degree-days: One equation, two interpretations. *Agricultural and Forest Meteorology* 87(1): 291–300.

Pebesma EJ and Bivand RS (2005) Classes and methods for spatial data in R. Available at: https://cran.r-project.org/doc/Rnews/.

Piao S, Liu Z, Wang T et al. (2017) Weakening temperature control on the interannual variations of spring carbon uptake across northern lands. *Nature Climate Change* 7: 359–363.

Polgar CA and Primack RB (2011) Leaf-out phenology of temperate woody plants: From trees to ecosystems. *New Phytologist* 191: 926–941.

R Core Team (2019) R: A language and environment for statistical computing. Vienna, Austria: R foundation for statistical computing. Available at: https://www.r-project.org/.

Royer DL (2001) Stomatal density and stomatal index as indicators of paleoatmospheric CO_2 concentration. *Review of Palaeobotany and Palynology* 114(1–2): 1–28.

Shepard D (1964) A two-dimensional interpolation for irregularly-spaced data function. In: *Proceedings of the 1968 23rd ACM national conference (ACM '68)*, New York, 27–29 August, pp. 517–524. New York: ACM.

Steinthorsdottir M, Elliott-Kingston C and Bacon KL (2018) Cuticle surfaces of fossil plants as a potential proxy for volcanic SO_2 emissions: Observations from the Triassic–Jurassic transition of East Greenland. *Palaeobiodiversity and Palaeoenvironments* 98(1): 49–69.

Vaarama A and Valanne T (1973) On the taxonomy, biology and origin of Betula tortuosa Ledeb. *Kevo Subarctic Research Station* 10: 70–84.

Van Oldenborgh GJ, Drijfhout S, Van Ulden A et al. (2009) Western Europe is warming much faster than expected. *Climate of the Past* 5(1): 1–12.

Wagner-Cremer F and Lotter AF (2011) Spring-season changes during the Late Pleniglacial and Bølling/Allerød interstadial. *Quaternary Science Reviews* 30(15–16): 1825–1828.

Wagner-Cremer F, Finsinger W and Moberg A (2010) Tracing growing degree-day changes in the cuticle morphology of Betula nana leaves: A new micro-phenological palaeo-proxy. *Journal of Quaternary Science* 25(6): 1008–1017.

Wagner-Cremer F, Kouwenberg LLR, Van Hoof TB et al. (2004) Reproducibility of Holocene atmospheric CO_2 records based on stomatal frequency. *Quaternary Science Reviews* 23(18–19): 1947–1954.

Wagner-Cremer F, Neuvonen S, Kürschner WM et al. (2000) The influence of hybridization on epidermal properties of birch species and the consequences for palaeoclimatic interpretations. *Plant Ecology* 148(1): 61–69.

Wagner-Cremer F, Visscher H, Kurschner WM et al. (2007) Influence of ontogeny and atmospheric CO_2 on stomata parameters of Osmunda regalis. *CFS Courier Forschungsinstitut Senckenberg* 258: 183–189.

Weijers S, Wagner-Cremer F, Sass-Klaassen U et al. (2013) Reconstructing high Arctic growing season intensity from shoot length growth of a dwarf shrub. *The Holocene* 23(5): 721–731.

Wickham H (2016) *ggplot2: Elegant Graphics for Data Analysis*. New York: Springer-Verlag.

Zohner CM and Renner SS (2014) Common garden comparison of the leaf-out phenology of woody species from different native climates, combined with herbarium records, forecasts long-term change. *Ecology Letters* 17(8): 1016–1025.

Zohner CM, Benito BM, Svenning JC et al. (2016) Day length unlikely to constrain climate-driven shifts in leaf-out times of northern woody plants. *Nature Climate Change* 6(12): 1120–1123.